A C^1 Virtual Element Method
on polyhedral meshes

L. Beirão da Veiga[a,b], F. Dassi[a], A. Russo[a,b]

[a]*Department of Mathematics and Applications, University of Milano - Bicocca,*
Via Cozzi 53, I-20153, Milano (Italy)
[b]*IMATI-CNR, 27100 Pavia (Italy)*

Abstract

The purpose of the present paper is to develop C^1 Virtual Elements in three dimensions for linear elliptic fourth order problems, motivated by the difficulties that standard conforming Finite Elements encounter in this framework. We focus the presentation on the lowest order case, the generalization to higher orders being briefly provided in the Appendix. The degrees of freedom of the proposed scheme are only 4 per mesh vertex, representing function values and gradient values. Interpolation error estimates for the proposed space are provided, together with a set of numerical tests to validate the method at the practical level.

Keywords: Virtual Element Method, polyhedral meshes, bi-Laplacian problem, C^1 regularity

1. Introduction

Fourth order partial differential equations are used to describe many different physical phenomena such as plate bending problems and evolution of transition interfaces. In standard H^2 conforming finite elements these problems require a globally C^1 piecewise polynomial space and, to get such regularity on a general unstructured partition, a very high minimal polynomial degree is needed. In [57] there is an analysis on the minimal degree required to build a finite element space in the Sobolev space $H^m(\mathbb{R}^d)$ via the Finite Element Method. In particular, the authors show that for H^2 the minimal polynomial degree is 5 in two dimensions and 9 in three dimensions. It is easy to understand that such compulsory high polynomial degree increases the computational effort and makes the method unpractical in many situations. For instance, a conforming C^1 finite element

Email addresses: `lourenco.beirao@unimib.it` (L. Beirão da Veiga),
`franco.dassi@unimib.it` (F. Dassi), `alessandro.russo@unimib.it` (A. Russo)

space on a tetrahedral mesh will require 220 degrees of freedom per element [56]. To avoid this high computational effort, there are possible alternatives in the literature, such as non-conforming and discontinuous schemes (see for instance [49, 26, 34, 50]), making use of a mixed formulation (see for instance [4, 35, 40, 45]) or construct more complex discrete spaces obtained by some macro-element strategy (see for instance [42, 60, 44]). It must be mentioned that C^1 finite elements are also important because they can be used to build exact discrete Stokes complexes, see for instance [41, 55] and the citations thereof.

Another strategy to get a conforming discrete approximation space in H^2 is to follow the recently born Virtual Element Method (VEM). The VEM is a novel generalization of the finite element method, introduced in [12, 8], that allows to use general polygonal/polyhedral meshes and which has been already succesfully applied to a large number of problems (a very brief list being [2, 20, 38, 37, 46, 10, 19, 31, 15, 59, 21, 24, 29, 30, 54, 36, 17, 32, 51, 13, 6, 5, 27]). The Virtual Element Method is not restricted to piecewise polynomials but avoids nevertheless the explicit integration of non-polynomial shape functions by a wise choice of the degrees of freedom and an innovative construction of the stiffness matrix. Although the main motivation of VEM is the use of general polytopal partitions, its flexibility can lead also to different advantages. One, initiated in [28, 18] and further investigated in [3, 11, 47, 48], is the possibility to develop C^1 conforming spaces, still keeping the accuracy order and the number of degrees of freedom at a reasonable level. More specifically, the lowest degree requires only three degrees of freedom for each vertex independently for the shape of the elements.

Since all the papers above are limited to the two-dimensional case, the purpose of the present contribution is to develop C^1 Virtual Elements in three dimensions. We focus the presentation on the lowest order case (the generalization to higher orders being briefly provided in the Appendix) for the sake of exposition but also since we believe this is the most interesting choice in practice. Developing a discrete Virtual Element space in three dimensions needs first the construction of ad-hoc two dimensional spaces on the faces (polygons) of the polyhedra, one for the function values and one for the normal derivatives. The final degrees of freedom of the proposed scheme are simply 4 per mesh vertex, representing function values and gradient component values. Consequently, although VEM can be applied to general polyhedral meshes, the proposed method becomes appealing also for standard tetrahedral meshes. After developing the method and the associated degrees of freedom, we prove interpolation estimates for the provided discrete space in standard L^2, H^1 and H^2 Sobolev norms. Finally, we show a set of numerical tests on classical linear fourth order elliptic problems that validate the method at the practical level. We also include a comparison, for the standard Poisson problem, with the C^0 VEM in 3D. It is finally worth noticing that, although the present paper is focused on the linear elliptic case, the presented discrete space could be used also to discretize more complex nonlinear problems, such as the Cahn-Hilliard equation.

The paper is organized as follows. In Section 2 we outline the range of fourth order linear problems under consideration. In Section 3 we describe the C^1 virtual element spaces and provide a set of associated degrees of freedom. In Section 4 we present the numerical method, that is the VE discretization of the problem. In Section 5, we prove the interpolation and convergence estimates. In Section 6, we present the numerical results. Finally, in Appendix A we briefly

outline the extension to the higher order case.

2. Continuous Problem

Let $\Omega \subset \mathbb{R}^3$ be a bounded domain, we consider the following problem: find $u(\mathbf{x}) : \Omega \to \mathbb{R}$ such that

$$\begin{cases} c_1 \Delta^2 u - c_2 \, \Delta u + c_3 \, u &=& f & \text{in } \Omega \\ u &=& g_1 & \text{on } \partial\Omega \\ \partial_n u &=& g_2 & \text{on } \partial\Omega \end{cases} \quad , \tag{1}$$

where $c_1 > 0$, $c_2, c_3 \geq 0$ are constant coefficients, $f \in L^2(\Omega)$ is the forcing term, $\partial_n u$ is the partial derivative of u with respect to the boundary normal $\mathbf{n}$, $g_1 \in H^{3/2}(\partial\Omega)$ and $g_2 \in H^{1/2}(\partial\Omega)$ are the Dirichlet data. Note that we have considered Dirichlet boundary conditions only for simplicity of exposition, the extension to more general cases is trivial. To define the variational formulation of Problem (1), we introduce the bilinear forms

$$\begin{aligned} a^\Delta(v, \, w) &:= \int_\Omega \nabla^2 v \, : \, \nabla^2 w \; \mathrm{d}\Omega & \forall v, \, w \in H^2(\Omega) \,, \\ a^\nabla(v, \, w) &:= \int_\Omega \nabla v \, \cdot \, \nabla w \; \mathrm{d}\Omega & \forall v, \, w \in H^1(\Omega) \,, \\ a^0(v, \, w) &:= \int_\Omega v \, w \; \mathrm{d}\Omega & \forall v, \, w \in L^2(\Omega) \,, \end{aligned} \tag{2}$$

where all the previous symbols refers to the standard notation for functional spaces. We define

$$V(\Omega) := \left\{ v \in H^2(\Omega) \, : \, v = g_1 \quad \text{and} \quad \partial_n u = g_2 \quad \text{on } \partial\Omega \right\},$$

and

$$V_0(\Omega) := \left\{ v \in H^2(\Omega) \, : \, v = 0 \quad \text{and} \quad \partial_n u = 0 \quad \text{on } \partial\Omega \right\}.$$

The weak formulation of Problem (1) reads: find $u \in V(\Omega)$ such that

$$c_1 \, a^\Delta(u, \, v) + c_2 \, a^\nabla(u, \, v) + c_3 \, a^0(u, \, v) = (f, \, v)_\Omega \qquad \forall v \in V_0(\Omega) \,, \tag{3}$$

where $(\cdot, \cdot)_\Omega$ is the standard L^2-inner product. Due to the coercivity of $a^\Delta(\cdot, \cdot)$ on the space $V_0(\Omega)$ the Lax-Milgram lemma yields the well posedness of the above problem.

Remark 2.1. *The method proposed in this paper can be applied also to second order elliptic problems (that is $c_1 = 0$ and $c_2 > 0$) to get a C^1 conforming solution, as shown in the numerical test in Section 6.6.*

Remark 2.2. *The method of the present paper can be extended to the variable coefficient case by combining this construction with the approach in [15, 14].*

3. C^1 Virtual Element Spaces

Let Ω_h be a discretization of Ω composed by polyhedrons. As in the standard VEM framework, we define the local space and projection operators in a generic polyhedron P and then we glue such local virtual element spaces to define the discrete global space, $V_h(\Omega_h)$.

We achieve this goal in two steps. We first define virtual spaces on faces, Sections 3.1 and 3.2, then we define virtual spaces on polyhedrons in Section 3.3. Since the virtual face spaces essentially correspond to 2D virtual spaces already defined in [12, 18, 61], we only make a brief review and refer to such papers for a deeper description.

In order to derive the convergence theory, we will need the following assumptions on the mesh Ω_h:

(**A1**) Each element P is star shaped with respect to a ball B_P whose radius is uniformly comparable with the polyhedron diameter, h_P.

(**A2**) Each face f is star shaped with respect to a disc B_f whose radius is uniformly comparable with the face diameter, h_f.

(**A3**) Given a polyhedron P all its edge lengths and face diameters are uniformly comparable with respect to its diameter h_P.

Remark 3.1. *It is easy to check that under assumptions (A1), (A2) and (A3) each polyhedron is the union of uniformly shape-regular tetrahedrons all sharing a central vertex.*

Let $\mathcal{D} \subset \mathbb{R}^d$, from now we refer to the polynomial space in d-variables of degree lower or equal to k as $\mathbb{P}_k(\mathcal{D})$.

3.1. Virtual element nodal space $V_h^\nabla(f)$

We define the preliminary space on each face $f \in \partial P$

$$\widetilde{V}_h^\nabla(f) := \left\{ v_h \in H^1(f) \quad : \quad \Delta_\tau v_h \in \mathbb{P}_0(f), \right.$$
$$\left. v_h|_{\partial f} \in C^0(\partial f), \, v_h|_e \in \mathbb{P}_1(e) \ \forall e \in \partial f \right\}.$$

where Δ_τ is the Laplace operator in the local face variables.

We consider the standard VEM setting proposed in [12] and we build the projection operator $\Pi_f^\nabla : \widetilde{V}_h^\nabla(f) \to \mathbb{P}_1(f)$, defined by

$$\begin{cases} a_f^\nabla(\Pi_f^\nabla v_h, p_1) & = a_f^\nabla(v_h, p_1) \quad \forall p_1 \in \mathbb{P}_1(f) \\ (\Pi_f^\nabla v_h, 1)_{\partial f} & = (v_h, 1)_{\partial f} \end{cases}, \tag{4}$$

where

$$a_f^\nabla(v_h, w_h) \quad := \quad \int_f \nabla_\tau v_h \cdot \nabla_\tau w_h \, df,$$

here ∇_τ is the gradient operator in the local face coordinates and $(\cdot, \cdot)_{\partial f}$ is the standard L^2 inner product over the boundary of f.

The projection operator Π_f^∇ is well defined and uniquely determined by the values of the function v_h at the vertices of the face f [12].

Moreover, starting from the space $\widetilde{V}_h^\nabla(f)$ and the projection operator Π_f^∇, we are able to define the nodal space

$$V_h^\nabla(f) := \left\{ v_h \in \widetilde{V}_h^\nabla(f) \ : \ \int_f \Pi_f^\nabla v_h \, \mathrm{d}f = \int_f v_h \, \mathrm{d}f \right\}, \tag{5}$$

whose degrees of freedom are the values of v_h at the vertices of f [12, 1].

3.2. Virtual element C^1 space $V_h^\Delta(f)$

We start from the preliminary space

$$\widetilde{V}_h^\Delta(f) := \left\{ v_h \in H^2(f) \quad : \quad \begin{aligned} &\Delta_\tau^2 v_h \in \mathbb{P}_1(f), \\ &v_h|_{\partial f} \in C^0(\partial f), \ v_h|_e \in \mathbb{P}_3(e) \ \forall e \in \partial f, \\ &\nabla_\tau v_h|_{\partial f} \in [C^0(\partial f)]^2, \ \partial_{n_e} v_h \in \mathbb{P}_1(e) \ \forall e \in \partial f \end{aligned} \right\},$$

where $\partial_{n_e} v_h$ denotes the outward normal derivative to each edge.

We consider the projection operator $\Pi_f^\Delta : \widetilde{V}_h^\Delta(f) \to \mathbb{P}_2(f)$ defined by the following relations

$$\begin{cases} a_f^\Delta \left(\Pi_f^\Delta v_h, p_2 \right) = a_f^\Delta (v_h, p_2) & \forall p_2 \in \mathbb{P}_2(f) \\ \left(\Pi_f^\Delta v_h, p_1 \right)_{\partial f} = (v_h, p_1)_{\partial f} & \forall p_1 \in \mathbb{P}_1(f) \end{cases}, \tag{6}$$

where

$$a_f^\Delta (v_h, w_h) \ := \ \int_f \nabla_\tau^2 v_h : \nabla_\tau^2 w_h \, \mathrm{d}f,$$

is a bilinear operator and ∇_τ^2 refers to the Hessian in the face local coordinates system.

The projection operator $\Pi_f^\Delta : \widetilde{V}_h^\Delta(f) \to \mathbb{P}_2(f)$ is well-defined and it is uniquely determined by the values of the function, $v_h(\nu)$, and the values of the gradient, $\nabla_\tau v_h(\nu)$, at the face vertices [3, 18, 61].

We exploit the space $\widetilde{V}_h^\Delta(f)$ and the projection operator Π_f^Δ to define the virtual element C^1 space

$$V_h^\Delta(f) := \left\{ v_h \in \widetilde{V}_h^\Delta(f) \ : \ \int_f \Pi_f^\Delta v_h \, p_1 \, \mathrm{d}f = \int_f v_h \, p_1 \, \mathrm{d}f, \quad \forall p_1 \in \mathbb{P}_1(f) \right\}. \tag{7}$$

A set of degrees of freedom for $V_h^\Delta(f)$ is given by the function and the function gradient values at the face vertices [18, 3].

Remark 3.2. *We would like to underline that the additional properties on face integrals required by the spaces $V_h^\nabla(f)$ and $V_h^\Delta(f)$, namely*

$$\int_f v_h \, \mathrm{d}f = \int_f \Pi_f^\nabla v_h \, \mathrm{d}f, \qquad \forall v_h \in V_h^\nabla(f) \tag{8}$$

5

and

$$\int_f v_h \, p_1 \, \mathrm{d}f = \int_f \Pi_f^\Delta v_h \, p_1 \, \mathrm{d}f \qquad \forall p_1 \in \mathbb{P}_1(f) , \qquad \forall v_h \in V_h^\Delta(f) \qquad (9)$$

will be essential to define our virtual scheme on polyhedrons.

Finally, we make use of the L^2-projection operator on faces $\boldsymbol{\Pi}_f^0 : [L^2(f)]^2 \to [\mathbb{P}_0(f)]^2$ to approximate the gradient of a generic function $v_h \in V_h^\Delta(f)$. Such projection operator is defined by these relations

$$\int_f \boldsymbol{\Pi}_f^0 \left(\nabla_\tau v_h \right) \cdot \boldsymbol{c} \, \mathrm{d}f = \int_f \nabla_\tau v_h \cdot \boldsymbol{c} \, \mathrm{d}f , \qquad \forall \boldsymbol{c} \in [\mathbb{P}_0(f)]^2 . \qquad (10)$$

This projection operator is computable from the degrees of freedom of $V_h^\Delta(f)$. Indeed, let us consider the right hand side of Equation (10)

$$\int_f \nabla_\tau v_h \cdot \boldsymbol{c} \, \mathrm{d}f = \int_{\partial f} v_h \left(\mathbf{n}_f \cdot \boldsymbol{c} \right) \mathrm{d}f = \sum_{e \in \partial f} \left(\mathbf{n}_e \cdot \boldsymbol{c} \right) \int_e v_h \, \mathrm{d}e ,$$

the last integral is *exactly* computable since the virtual function v_h is a polynomial of degree 3 on the edges and such edge polynomials are uniquely determined by the degrees of freedom of $V_h^\Delta(f)$.

3.3. Virtual element space in P

Given a polyhedron $P \in \Omega_h$ we consider the preliminary space

$$\widetilde{V}_h(P) := \left\{ v_h \in H^2(P) \quad : \quad \Delta^2 v_h \in \mathbb{P}_2(P), \right.$$
$$v_h|_{S_P} \in C^0(S_P) , \nabla v_h|_{S_P} \in [C^0(S_P)]^3 ,$$
$$\left. v_h|_f \in V_h^\Delta(f) , \partial_{n_f} v_h|_f \in V_h^\nabla(f) \quad \forall f \in \partial P \right\} ,$$
$$(11)$$

where S_P denotes the skeleton (the union of all edges) of the polyhedron P.

This space is composed by functions whose bi-Laplacian is a polynomial of degree 2. The restriction of such functions on each face is a two dimensional C^1 virtual function, see Section 3.2, while their normal derivative on each face is a C^0 virtual function, see Section 3.1.

To build a suitable virtual element space in a polyhedron P, we define two sets of linear operators from $\widetilde{V}_h(P)$ to $\mathbb{R}$:

D0: the values of the function at the vertices, $v_h(\nu)$;

D1: the values of the gradient components at the vertices, $\nabla v_h(\nu)$.

We define the projection operator $\Pi_P^\Delta : \widetilde{V}_h(P) \to \mathbb{P}_2(P)$ by the following relations

$$\begin{cases} a_P^\Delta \left(\Pi_P^\Delta v_h , p_2 \right) = a_P^\Delta \left(v_h , p_2 \right) & \forall p_2 \in \mathbb{P}_2(P) \\ \left(\Pi_P^\Delta v_h , p_1 \right)_{\partial P} = \left(v_h , p_1 \right)_{\partial P} & \forall p_1 \in \mathbb{P}_1(P) \end{cases} , \qquad (12)$$

where we introduced

$$a_P^\Delta \left(v_h\, , w_h\right) \quad := \quad \int_P \nabla^2 \, v_h \, : \nabla^2 \, w_h \, \mathrm{dP}\,, \tag{13}$$

and $(\cdot,\cdot)_{\partial P}$ is the standar L^2 inner product over the boundary of P.

As usual in VEM, the second condition in Equation (12) is needed to select an element from the non-trivial kernel of the operator $a^\Delta(\cdot,\cdot)_P$.

Lemma 3.1. *The operator $\Pi_P^\Delta : \widetilde{V}_h(P) \to \mathbb{P}_2(P)$ is computable and uniquely determined by the values of the linear operators **D0** and **D1**.*

Proof. Let us consider the first condition in Equation (12). The main issue is how to compute the right hand side since it involves the virtual function v_h. We integrate by parts and we get

$$\begin{aligned}
a_P^\Delta\left(v_h\, , p_2\right) & = & \int_P \nabla^2 \, v_h \, : \nabla^2 p_2 \, \mathrm{dP} = \\
& = & -\int_P \nabla\, v_h \cdot \mathbf{div}(\nabla^2 p_2)\, \mathrm{dP} + \int_{\partial P} \nabla\, v_h \cdot \left[(\nabla^2 p_2)\, \mathbf{n}\right] \mathrm{d}f = \\
& = & \sum_{f\in\partial P} \int_f \nabla\, v_h \cdot \left[(\nabla^2 p_2)\, \mathbf{n}_f\right] \mathrm{d}f\,.
\end{aligned}$$

Then, we make the following orthonormal vector decomposition

$$\nabla\, v_h = (\nabla\, v_h \cdot \mathbf{v}_{f,\widetilde{x}})\, \mathbf{v}_{f,\widetilde{x}} + (\nabla\, v_h \cdot \mathbf{v}_{f,\widetilde{y}})\, \mathbf{v}_{f,\widetilde{y}} + (\nabla\, v_h \cdot \mathbf{n}_f)\, \mathbf{n}_f\,,$$

where $\mathbf{v}_{f,\widetilde{x}}$ and $\mathbf{v}_{f,\widetilde{y}}$ are three dimensional unit vectors (tangent to the face) which identify the local two dimensional coordinate system of f, and $\mathbf{n}_f$ is the outward pointing normal of the face, see Figure 1. We plug this decomposition in the previous equation and we get

$$\begin{aligned}
a_P^\Delta\left(v_h\, , p_2\right) & = & \sum_{f\in\partial P} \left[\omega_{\mathbf{v}_{f,\widetilde{x}}} \int_f (\nabla\, v_h \cdot \mathbf{v}_{f,\widetilde{x}})\, \mathrm{d}f + \omega_{\mathbf{v}_{f,\widetilde{y}}} \int_f (\nabla\, v_h \cdot \mathbf{v}_{f,\widetilde{y}})\, \mathrm{d}f + \right. \\
& & \left. + \omega_{\mathbf{n}_f} \int_f (\nabla\, v_h \cdot \mathbf{n}_f)\, \mathrm{d}f\right],
\end{aligned} \tag{14}$$

where

$$\omega_{\mathbf{v}_{f,\widetilde{x}}} := \mathbf{v}_{f,\widetilde{x}} \cdot \left[(\nabla^2 p_2)\, \mathbf{n}_f\right], \qquad \omega_{\mathbf{v}_{f,\widetilde{y}}} := \mathbf{v}_{f,\widetilde{y}} \cdot \left[(\nabla^2 p_2)\, \mathbf{n}_f\right],$$

and

$$\omega_{\mathbf{n}_f} := \mathbf{n}_f \cdot \left[(\nabla^2 p_2)\, \mathbf{n}_f\right],$$

are constant values so we can move them out from the integral over the face f. Then, the integrals in Equation (14) are computable using the face projectors of the previous Sections, which in turn are uniquely defined by the values of **D0** and **D1**. More specifically, since for (11) we have $(\nabla\, v_h \cdot \mathbf{n}_f) \in V_h^\nabla(f)$, we can exploit the standard nodal projection Π_f^∇ and condition (8). Furthermore, since both $(\nabla\, v_h \cdot \mathbf{v}_{f,\widetilde{x}})$ and $(\nabla\, v_h \cdot \mathbf{v}_{f,\widetilde{y}})$ correspond to tangent derivatives of $v_h|_f$ and $v_h|_f \in V_h^\Delta(f)$ those integrals can be computed using (10). Finally, the last condition of Equation (12) involves only integrals on faces of P and thus it is computable from **D0** and **D1** recalling property (9).
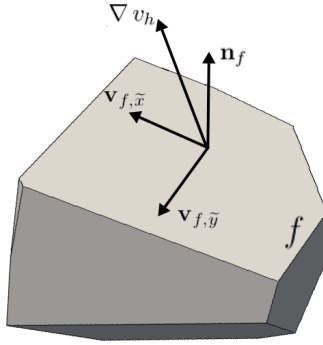
Figure 1: The unit vectors $\mathbf{v}_{f,\widetilde{x}}$, $\mathbf{v}_{f,\widetilde{y}}$ and $\mathbf{n}_f$ for the face f.

$\square$

Now we are ready to define the local virtual element space, $V_h(P)$

$$V_h(P) := \left\{ v_h \in \widetilde{V}_h(P) : \int_P \Pi_P^\Delta v_h \, p_2 \, \mathrm{dP} = \int_P v_h \, p_2 \, \mathrm{dP}, \ \forall p_2 \in \mathbb{P}_2(P) \right\}. \quad (15)$$

It is trivial to check that

$$\mathbb{P}_2(P) \subseteq V_h(P).$$

Lemma 3.2. *The set of linear operators **D0** and **D1** are a set of degrees of freedom for the space $V_h(P)$.*

Proof. A function $w_h \in \widetilde{V}_h(P)$ is the solution of a well-posed bi-Laplacian problem defined in P, whose forcing term is a polynomial of degree 2,

$$\Delta^2 w_h \in \mathbb{P}_2(P), \quad (16)$$

and its Dirichlet boundary data are

$$w_h|_f \in V_h^\Delta(f), \quad \partial_{n_f} w_h|_f \in V_h^\nabla(f) \quad \forall f \in \partial P. \quad (17)$$

First of all, recalling the definition of the face spaces and their associated degrees of freedom, it is easy to check that **D0** and **D1** constitute a set of degrees of freedom for the boundary space $\widetilde{V}_h(P)|_{\partial P}$.

The dimension of $\widetilde{V}_h(P)$ is equal to the dimension of the data space, i.e. the dimension of the loading term plus the dimension of the boundary data space. In this particular case we have that

- the dimension of the loading term is 10 since we are dealing with polynomials of degree 2 in the three dimensional space and

- the dimension of the boundary data space is given by the sum of the cardinality of **D0** and **D1**, $\#\{\mathbf{D0}\} + \#\{\mathbf{D1}\}$.

We know that $V_h(P)$ is a subspace of $\widetilde{V}_h(P)$ obtained by imposing

$$\int_P \Pi_P^\Delta v_h \; p_2 \, \mathrm{dP} = \int_P v_h \; p_2 \, \mathrm{dP} \qquad \forall p_2 \in \mathbb{P}_2(P) \,, \tag{18}$$

which can be re-written as a set of 10 linear equations. We deduce that

$$\dim(V_h(P)) \geq \dim(\widetilde{V}_h(P)) - 10 = \#\{\mathbf{D0}\} + \#\{\mathbf{D1}\} \,.$$

Therefore, once we prove that a generic function $v_h \in V_h(P)$ with vanishing $\mathbf{D0}$ and $\mathbf{D1}$ values is the zero element of $V_h(P)$, we deduce that

$$\dim(V_h(P)) = \#\{\mathbf{D0}\} + \#\{\mathbf{D1}\} \,,$$

and this will complete the proof.

To achieve this goal, suppose that $v_h \in V_h(P)$ vanishes on $\mathbf{D0}$ and $\mathbf{D1}$. Then

$$v_h|_f = 0, \quad \text{and} \quad \partial_{n_f} v_h|_f = \mathbf{0} \qquad \forall f \in \partial P \,.$$

Moreover, since $\mathbf{D0}$ and $\mathbf{D1}$ are zero, we have that $\Pi^\Delta v_h = 0$, Lemma 3.1, and therefore, recalling (15),

$$\int_P v_h \; p_2 \, \mathrm{dP} = \int_P \Pi_P^\Delta v_h \; p_2 \, \mathrm{dP} = 0 \qquad \forall p_2 \in \mathbb{P}_2(P) \,. \tag{19}$$

Since $v_h \in V_h(P)$, by definition $\Delta^2 v_h \in \mathbb{P}_2(P)$. Consequently, we can take $\Delta^2 v_h$ as a test function p_2 in Equation (19). Then, if we integrate by parts two times and we exploit the fact that on the boundary v_h and $\partial_n v_h$ are null, we get

$$0 = \int_P v_h \, \Delta^2 v_h \, \mathrm{dP} = \int_P \Delta v_h \, \Delta v_h \, \mathrm{dP} \quad \Rightarrow \quad \Delta v_h = 0 \,.$$

Thus, since v_h is zero on the boundary and its Laplacian is null, v_h is the null function.

$\square$

To set up the discrete form of Problem (3), the projector operator Π_P^Δ alone is not sufficient, we also need an L^2-projection operator Π_P^0 and an H^1-projection operator Π_P^∇.

Let us start with $\Pi_P^0 : V_h(P) \to \mathbb{P}_2(P)$. This projection operator is determined by the following conditions:

$$a_P^0(\Pi_P^0 v_h, \, p_2) = a_P^0(v_h, \, p_2) \quad \forall p_2 \in \mathbb{P}_2(P) \,, \tag{20}$$

where we defined the bilinear form

$$a_P^0(v_h, \, w_h) := \int_P v_h \, w_h \, \mathrm{dP} \,. \tag{21}$$

The subsequent lemma easily follows recalling (15) and the computability of Π_P^Δ.

Lemma 3.3. *The projection operator $\Pi_P^0 : V_h(P) \to \mathbb{P}_2(P)$ is computable from $\mathbf{D0}$ and $\mathbf{D1}$ (and actually coincides with Π_P^Δ, see (15)).*

Now we consider the projection operator $\Pi_P^\nabla : V_h(P) \to \mathbb{P}_2(P)$ defined by

$$
\begin{cases}
a_P^\nabla \left(\Pi_P^\nabla v_h \, , p_2 \right) & = a_P^\nabla \left(v_h \, , p_2 \right) \quad \forall p_2 \in \mathbb{P}_2(P) \\
a_P^0 \left(\Pi_P^\nabla v_h \, , 1 \right) & = a_P^0 \left(v_h \, , 1 \right)
\end{cases}
, \tag{22}
$$

where

$$
a_P^\nabla \left(v_h \, , w_h \right) := \int_P \nabla v_h \cdot \nabla w_h \, \mathrm{d}P . \tag{23}
$$

Lemma 3.4. *The projection operator $\Pi_P^\nabla : V_h(P) \to \mathbb{P}_2(P)$ is computable from* **D0** *and* **D1**.

Proof. We have to check that the right hand side of the first equation in (22) is computable using only the degrees of freedom values **D0** and **D1**. Let us consider the first condition in (22). If we integrate by parts and recall definitions (7) and (15), we notice that this term depends *only* on the projection operators Π_P^0 and $\Pi_f^\triangle$, that in turn depend only on **D0** and **D1** values. Indeed

$$
\begin{aligned}
a_P^\nabla \left(v_h \, , p_2 \right) & = \int_P \nabla v_h \cdot \nabla p_2 \, \mathrm{d}P \\
& = -\int_P v_h \, \Delta p_2 \, \mathrm{d}P + \int_{\partial P} v_h \left(\nabla p_2 \cdot \mathbf{n} \right) \mathrm{d}f \\
& = -\Delta p_2 \int_P v_h \, \mathrm{d}P + \sum_{f \in \partial P} \int_f v_h \left(\nabla p_2 \cdot \mathbf{n}_f \right) \mathrm{d}f \\
& = -\Delta p_2 \int_P \Pi_P^0 v_h \, \mathrm{d}P + \sum_{f \in \partial P} \int_f \Pi_f^\triangle v_h \left(\nabla p_2 \cdot \mathbf{n}_f \right) \mathrm{d}f .
\end{aligned}
$$

$\square$

3.4. Global virtual space $V_h(\Omega_h)$

The global discrete space which will be used to discretize Problem (3) is

$$
V_h(\Omega_h) := \{ v_h \in V(\Omega) \ : \ v_h|_P \in V_h(P) \} . \tag{24}
$$

Let us consider the canonical basis functions $\{\phi_i\}_i$ associated with the degrees of freedom **D0** and **D1**, i.e. the functions ϕ_i which take value 1 on the $i-$th degree of freedom and vanish for the remaining ones. It is easy to check that, assuming for simplicity a uniform mesh family, the basis functions associated with the set **D0** satisfy $\|\phi_i\|_{L^\infty(\Omega)} \sim 1$, while the basis functions associated with **D1** behave like $\|\phi_i\|_{L^\infty(\Omega)} \sim h_P$, where h_P is the diameter of the polyhedron P. Since this different scaling behavior with respect to the mesh size may yield detrimental effects on the condition number of the discrete system it is wiser to scale accordingly the second set of degrees of freedom.

Consequently, the global degrees of freedom for $V_h(\Omega)$ which we adopt in practice are

$\mathcal{C}0$: evaluations of $v_h(\nu)$ at each vertex of the mesh Ω_h;

$\mathcal{C}1$: evaluations of $h_\nu \nabla v_h(\nu)$ at each vertex of the mesh Ω_h,

where h_ν denotes some local mesh size parameter, for instance the average diameter of the neighboring elements. This choice will be better discussed in Section 6.5. The dimension of $V_h(\Omega_h)$ is four times the number of mesh vertices.

4. Discrete virtual forms and the discrete problem

When we are solving a PDE via the virtual element method, we have to define a suitable set of discrete forms for the problem at hand. Such forms are constructed element-by-element and depend only on the local degrees of freedom **D0** and **D1**, also via the projection operators Π_P^Δ, Π_P^0 and Π_P^∇.

Let $P \in \Omega_h$ and $v_h, w_h \in V_h(\Omega_h)$, we define the following strictly positive bilinear form $s_P : V_h(P) \times V_h(P) \to \mathbb{R}$,

$$s_P(v_h, w_h) := \sum_{\nu \in P} \left(v_h(\nu)\, w_h(\nu) + \left(h_\nu\, \nabla v_h(\nu) \right) \cdot \left(h_\nu \nabla w_h(\nu) \right) \right), \qquad (25)$$

where ν is a generic vertex of the polyhedron P and h_ν is the scaling parameter, see the definition of the degrees of freedom $\mathcal{C}0$ and $\mathcal{C}1$. Recalling the continuous global form in Equation (2) and the local bilinear operators defined in Equations (13), (21) and (23), we construct the following local discrete linear forms

$$
\begin{aligned}
a_{h,P}^\Delta(v_h, w_h) &:= a_P^\Delta(\Pi_P^\Delta v_h, \Pi_P^\Delta w_h) \;+\; h_P^{-1} s_P(v_h - \Pi_P^\Delta v_h, w_h - \Pi_P^\Delta w_h), \\
a_{h,P}^\nabla(v_h, w_h) &:= a_P^\nabla(\Pi_P^\nabla v_h, \Pi_P^\nabla w_h) \;+\; h_P\; s_P(v_h - \Pi_P^\nabla v_h, w_h - \Pi_P^\nabla w_h), \\
a_{h,P}^0(v_h, w_h) &:= a_P^0(\Pi_P^0 v_h, \Pi_P^0 w_h) \;+\; h_P^3\; s_P(v_h - \Pi_P^0 v_h, w_h - \Pi_P^0 w_h),
\end{aligned}
$$
$$\qquad (26)$$

for all $v_h, w_h \in V_h(P)$, where h_P is the diameter of the polyhedron P. The construction above is standard in VEM, see for instance [12, 8]. The first term of each bilinear form in Equation (26) is the so-called consistency part, while the second term is the stability part. This stability part is scaled in such a way that, under the assumptions (A1)-(A3), there exist two positive constants $c^\star, c_\star$ such that

$$c_\star a_P^\sharp(v_h, v_h) \leq a_{h,P}^\sharp(v_h, v_h) \leq c^\star a_P^\sharp(v_h, v_h) \quad \forall v_h \in V_h(P), \qquad (27)$$

where, as before, the symbol $\sharp$ stands for Δ, ∇ and 0, respectively.

Lemma 4.1 (consistency). *For all the bilinear forms in Equation (26) it holds*

$$a_{h,P}^\sharp(v_h, p_2) = a_P^\sharp(v_h, p_2) \qquad \forall p_2 \in \mathbb{P}_2(P), \forall v_h \in V_h(P), \qquad (28)$$

where the symbol $\sharp$ stands for Δ, ∇ and 0, respectively.

Proof. The property in Equation (28) follows from the fact that the projection operators, Π_P^Δ, Π_P^∇, and Π_P^0, are orthogonal with respect to the bilinear form they are associated with.

$\square$

Lemma 4.1 states that the discrete bilinear forms $a_{h,P}^\sharp(\cdot, \cdot)$ are *exact* when one of the entries is a polynomials of degree 2. Finally, as in a standard virtual element framework, the global discrete forms are obtained by summing each local bilinear form over all mesh elements. Then the discrete problem reads: find $u_h \in V_h(\Omega_h)$ such that

$$c_1\, a_h^\Delta(u_h, v_h) + c_2\, a_h^\nabla(u_h, v_h) + c_3\, a_h^0(u_h, v_h) = (f_h, v_h)_{\Omega_h} \quad \forall v_h \in V_0(\Omega_h). \qquad (29)$$

where

$$(f_h,\, v_h)_{\Omega_h} := \sum_{P \in \Omega_h} \int_P \Pi_P^0 v_h \, f_h \, \mathrm{dP}\,.$$

Remark 4.1. *The scheme of the present paper can be immediately extended to the case where the Laplace operator is used instead of the Hessian operator in the definition of the fourth order bilinear form. The only modification is to substitute the form $a_P^\Delta(\cdot,\cdot)$ with*

$$a_P^\Delta(v,w) = \int_P \Delta v \, \Delta w \, \mathrm{d}P$$

and keep the same construction as in (26) for its discrete counterpart.

5. Interpolation and convergence estimates

In the present section we derive convergence estimates for the proposed method, under the geometric mesh assumptions (A1)-(A3) of the previous sections. In the sequel, the symbol $\lesssim$ will denote bounds up to a contant independent of h.

Theorem 5.1. *Let the mesh assumptions (A1)-(A3) hold. Let $u \in H^3(\Omega)$ be the solution of Problem (3) and u_h the solution of the corresponding discrete formulation (29). Then, it holds*

$$\|u - u_h\|_{2,\Omega} \le c\,h\,|u|_{3,\Omega}$$

To derive the proof, following the same identical steps as [12], Theorem 3.1, one gets the "best approximation" bound

$$\|u - u_h\|_{2,\Omega} \lesssim \|u - u_I\|_{2,\Omega} + \|u - u_\pi\|_{2,\Omega_h} + h^2 \|f\|_{0,\Omega}, \qquad (30)$$

for any interpolant $u_I \in V_h$ and piecewise $\mathbb{P}_2$-polynomial u_π, and where $|\cdot|_{s,\Omega_h}$ denotes a broken (with respect to the mesh) Sobolev norm of order s, $s \ge 0$.

The second term is immediately bounded by standard polynomial approximation estimates on star-shaped domains (see for instance [25]), yielding

$$\|u - u_\pi\|_{2,\Omega_h} \lesssim h\,|u|_{3,\Omega_h}\,.$$

Therefore, the main effort in proving Theorem 5.1 is bounding the first term in the right hand side of (30), that is showing the interpolation estimates for the space V_h. In order to do so, we will first prove interpolation estimates for the simpler space

$$W_h(\Omega_h) := \{ v_h \in V(\Omega) \,:\, v_h|_P \in W_h(P) \quad \forall P \in \Omega_h \}\,,$$

where

$$W_h(P) := \Bigg\{ v_h \in H^2(P) \quad:\quad \Delta^2 v_h = 0,$$
$$v_h|_{S_P} \in C^0(S_P)\,, \nabla v_h|_{S_P} \in [C^0(S_P)]^3\,,$$
$$v_h|_f \in V_h^\Delta(f)\,, \partial_{n_f} v_h|_f \in V_h^\nabla(f) \quad \forall f \in \partial P \Bigg\}\,,$$

Following the same arguments in Section 3.3, it is easy to check that the operators **D0** and **D1** constitute a set of degrees of freedom also for $W_h(P)$.

Remark 5.1. *By adding and subtracting a piecewise second-order polynomial, then using a triangle inequality and the continuity of Π_P^Δ in the H^2 norm, finally recalling standard approximation results for polynomials on star-shaped domains, from Theorem 5.1 one can easily derive also*

$$\sum_{P \in \Omega_h} \|u - \Pi_P^\Delta(u_h)\|_{2,P}^2 \le c\, h^2 |u|_{3,\Omega_h}^2$$

that states the convergence of the projected discrete solution.

5.1. Interpolation estimates for W_h

In deriving the estimates for the space W_h, we will take full advantage of known results for two-dimensional C^0 and C^1 VEM spaces (cited below). In addition, we will use the following standard results on the continuous dependence of the solution on the boundary biharmonic data in a polyhedron P (see for instance [39, 7]).

Given a polyhedron P, let r_1, r_2 be two scalar functions living on ∂P satisfying $r_1 \in C^0(\partial P)$ and $r_1 \in H^{3/2}(f)$, $r_2 \in H^{1/2}(f)$ for each face $f \in \partial P$. Consider the standard biharmonic Dirichlet problem

$$\begin{cases} \Delta^2 v = 0 & \text{in } P \\ v = r_1 & \text{on } \partial P \\ \partial_n v = r_2 & \text{on } \partial P \end{cases} \tag{31}$$

where all the operators are to be intended in weak sense. Below, $\mathbf{n}$ will denote the outward normal to the polyhedron's boundary (face by face).

Lemma 5.2. *Let the auxiliary three-dimensional vector field $\mathbf{r} = \nabla_\tau r_1 + \mathbf{n}\, r_2$ living on ∂P. Assume that such vector field $\mathbf{r}$ is (component-wise) in $H^{1/2}(\partial P)$. Then it holds*

$$|u|_{2,P} \le C |\mathbf{r}|_{1/2,\partial P}.$$

The constant C here above depends only on the star-shapedness of the polyhedron (the constant appearing in assumption (A1)-(A2)) and the Lipschitz constant of its boundary.

Note that the condition $\mathbf{r} \in [H^{1/2}(\partial P)]^3$ takes into account the necessary compatibility conditions at the edges. We can now state the following interpolation result for the W_h space.

Proposition 5.1. *Let $u \in H^3(\Omega)$ and w_I the only function in W_h that interpolates the nodal values of u and ∇u at all vertexes of Ω_h. Then it holds*

$$|u - w_I|_{2,\Omega} \lesssim h |u|_{3,\Omega_h}.$$

Proof. We prove a local interpolation estimate, the global one following immediately by summing over all the elements. Let $P \in \Omega_h$. We start by splitting the error $u - w_I = \widetilde{e} + \widehat{e}$ where

$$\Delta^2 \widetilde{e} = 0 \text{ in } P, \quad \widetilde{e} = u - w_I \text{ on } \partial P, \quad \partial_n \widetilde{e} = \partial_n(u - w_I) \text{ on } \partial P,$$
$$\Delta^2 \widehat{e} = \Delta^2(u - w_I) \text{ in } P, \quad \widehat{e} = 0 \text{ on } \partial P, \quad \partial_n \widehat{e} = 0 \text{ on } \partial P.$$

13

An integration by parts easily shows that

$$|u - w_I|^2_{2,P} = |\widehat{e}|^2_{2,P} + |\widetilde{e}|^2_{2,P}, \tag{32}$$

so that we need to bound the two terms above. For the first term, we again integrate by parts twice and obtain, also recalling that $\Delta^2 w_I = 0$ by definition of $W_h(P)$,

$$
\begin{aligned}
|\widehat{e}|^2_{2,P} &= \int_P (\Delta^2 \widehat{e}) \, \widehat{e} \, \mathrm{dP} \leq \|\Delta^2 \widehat{e}\|_{-1,P} \, \|\widehat{e}\|_{1,P} \\
&= \|\Delta^2 u\|_{-1,P} \, \|\widehat{e}\|_{1,P} \lesssim \|\Delta^2 u\|_{-1,P} \, |\widehat{e}|_{1,P},
\end{aligned}
$$

where in the last step we used a Poincaré inequality ($\widehat{e}$ vanishes on the boundary of P). The first multiplicative term in the right hand side is bounded by $|u|_{3,P}$ (to show this it is sufficient to apply the definition of dual norm and integrate once by parts). The second term corresponds to the L^2 norm of $\nabla \widehat{e}$, that is a (vector valued) function in $H^1(P)$ vanishing on the boundary (see definition of $\widehat{e}$). Therefore a scaled Poincaré inequality immediately yields

$$|\widehat{e}|^2_{2,P} \leq |u|_{3,P} \, \|\nabla \widehat{e}\|_{0,P} \lesssim h_P |u|_{3,P} \, |\widehat{e}|_{2,P} \tag{33}$$

that gives the desired bound for the first term in (32).

For the second term in (32), we make use of Lemma 5.2 and the definition of $\widetilde{e}$. Note that, due to the regularity of u and the definition of $W_h(P)$, the boundary data in the definition of $\widehat{e}$ satisfies the hypotheses of the Lemma. Moreover, it is trivial to check that the vector field $\mathbf{r}$ appearing in Lemma 5.2 in this case is nothing but $\nabla(u - w_I)$. Therefore we obtain the bound

$$|\widetilde{e}|^2_{2,P} \lesssim |\nabla(u - w_I)|^2_{1/2,\partial P}. \tag{34}$$

Note that the above bound is uniform (in P) since the elements P are star shaped and have uniformly bounded Lipschitz constant. Indeed, the observation in Remark 3.1 easily implies that each polyhedron P has a uniformly Lipschitz continuous boundary (actually, it holds also under the assumption (A1) alone, as shown in [23]).

By definition of the face spaces $V_h^\Delta(f)$ and $V_h^\nabla(f)$, the components of the vector field ∇w_I are in $H^1(f)$ for every face $f \in \partial P$. Since by definition of $W_h(P)$ the gradient of w_I is continuous on the skeleton, we have $\nabla w_I \in [H^1(\partial P)]^3$. Standard trace estimates, recalling $u \in H^3(P)$ imply an analogous property $\nabla u \in [H^1(\partial P)]^3$. Therefore, first by space interpolation theory and then summing on faces, from (35) we get

$$
\begin{aligned}
|\widetilde{e}|^2_{2,P} &\lesssim \|\nabla(u - w_I)\|_{0,\partial P} |\nabla(u - w_I)|_{1,\partial P} \\
&\lesssim \Big(\sum_{f \in \partial P} \|\nabla(u - w_I)\|^2_{0,f} \Big)^{1/2} \Big(\sum_{f \in \partial P} |\nabla(u - w_I)|^2_{1,f} \Big)^{1/2}.
\end{aligned} \tag{35}
$$

We note that, in both terms above, one can split for each face f

$$\nabla(u - w_I)|_f = (\nabla(u - w_I)|_f)_{\boldsymbol{\tau}} + (\nabla(u - w_I)|_f \cdot \mathbf{n}_f)\mathbf{n}_f \,,$$

that is the tangential and normal components of the vector $\nabla(u - w_I)|_f$. Therefore, for every face f

$$
\begin{aligned}
\|\nabla(u - w_I)\|_{0,f} &\leq \|(\nabla(u - w_I)|_f)_{\boldsymbol{\tau}}\|_{0,f} + \|\partial_n(u - w_I)\|_{0,f} \\
&= |u - w_I|_{1,f} + \|\partial_n u - \partial_n w_I\|_{0,f}
\end{aligned} \tag{36}
$$

and analogously

$$|\nabla(u - w_I)|_{1,f} \le |u - w_I|_{2,f} + |\partial_n u - \partial_n w_I|_{1,f}. \qquad (37)$$

We now need to recall that the restriction to faces of the space $W_h(P)$ corresponds, by definition, to C^1 virtual spaces in 2D [28, 18, 3] and that its normal derivative corresponds to C^0 virtual spaces in 2D [12, 1]. Therefore the bounds for the first term in the right-hand side of (36) and for the first term in the right-hand side of (37) follow from known interpolation theory for C^1 virtual spaces in 2D, see [11]. The bounds for the second term in the right-hand side of (36) and for the second term in the right-hand side of (37) follow from known interpolation theory for C^0 virtual spaces in 2D, see [16, 24]. Therefore, from (35) combined with (36)-(37), we get

$$\begin{aligned}
|\widetilde{e}|^2_{2,P} &\lesssim \Big(\sum_{f \in \partial P} h_f^3 |u|^2_{5/2,f} + h_f^3 |\partial_n u|^2_{3/2,f} \Big)^{1/2} \Big(\sum_{f \in \partial P} h_f |u|^2_{5/2,f} + h_f |\partial_n u|^2_{3/2,f} \Big)^{1/2} \\
&\lesssim h_P^2 |u|^2_{3,P},
\end{aligned}$$
$$(38)$$

where the last bound above follows from a (face by face) trace inequality. The local result now follows easily combining (32) with (33) and (38)

$$|u - w_I|_{2,P} \lesssim h_P |u|_{3,P} \qquad \forall P \in \Omega_h. \qquad (39)$$

$\square$

5.2. Interpolation estimates for V_h

We have the following result.

Proposition 5.2. *Let $u \in H^3(\Omega)$ and u_I the only function in V_h that interpolates the nodal values of u and ∇u at all vertexes of Ω_h. Then it holds*

$$|u - u_I|_{2,\Omega} \lesssim h |u|_{3,\Omega_h}.$$

Proof. Given $u \in H^3(\Omega)$, let w_I be its interpolant in W_h. We fix our attention on a generic polyhedron $P \in \Omega_h$, the global estimates will then follow from the local ones by summing over all elements. Moreover let the auxiliary space $Q = \mathbb{P}_2(P)$. Now we consider the following problem in mixed form

$$\begin{cases}
\text{Find } \varphi \in H_0^2(P), \ p \in Q \text{ such that} \\
\displaystyle\int_P \nabla^2 \varphi : \nabla^2 v \, \mathrm{d}P + \int_P p \, v \, \mathrm{d}P = 0 \qquad \forall v \in H_0^2(P) \\
\displaystyle\int_P \varphi \, q \, \mathrm{d}P = \int_P \big(\Pi_P^\Delta(w_I) - w_I \big) q \, \mathrm{d}P \qquad \forall q \in Q.
\end{cases} \qquad (40)$$

We endow the space Q with the norm

$$\|q\|_Q := h_P^2 \|q\|_{0,P} \quad \forall q \in Q.$$

Problem (40) is a standard problem in mixed form. Since the coercivity on the kernel is clearly guaranteed, in order to prove its well posedness we need only to check the inf-sup condition (see for instance [22]). Given any $q \in Q$, let T be any

one of the tetrahedra of Remark 3.1 and let b_T be the standard quartic bubble on T. Then, noting that $b_T^2 q \in H_0^2(P)$, standard properties of polynomials yield

$$\sup_{v \in H_0^2(P)} \frac{\int_P q\, v \, \mathrm{dP}}{|v|_{2,P}} \geq \frac{\int_T q\,(b_T^2 q)\, \mathrm{dP}}{|b_T^2 q|_{2,T}} \gtrsim \frac{\|q\|_{0,T}^2}{h_P^{-2}\|q\|_{0,T}} = h_P^2\|q\|_{0,T} \gtrsim h_P^2\|q\|_Q,$$

that is the inf-sup condition for problem (40). Since (40) is well posed, we have

$$
\begin{aligned}
|\varphi|_{2,P} &\lesssim \|\Pi_P^\Delta(w_I) - w_I\|_{Q^\star} = \sup_{q \in Q} \frac{\int_P \left(\Pi_P^\Delta(w_I) - w_I\right) q \, \mathrm{dP}}{h_P^2 \|q\|_{0,P}} \\
&\leq h_P^{-2}\|\Pi_P^\Delta(w_I) - w_I\|_{0,P}.
\end{aligned}
$$

Since by definition see (12)

$$\int_{\partial P} \left(\Pi_P^\Delta(w_I) - w_I\right) p_1 \, \mathrm{d}\partial\mathrm{P} = 0 \qquad \forall p_1 \in \mathbb{P}_1(P),$$

by a Poincaré-type inequality (the standard proof being omitted for the sake of brevity) the above bound becomes

$$|\varphi|_{2,P} \lesssim |\Pi_P^\Delta(w_I) - w_I|_{2,P}.$$

By a triangle inequality (and recalling that the operator Π_P^Δ is a projection operator onto $\mathbb{P}_2(P)$ minimizing the distance in the H^2 seminorm) the above bound leads to

$$
\begin{aligned}
|\varphi|_{2,P} &\lesssim |\Pi_P^\Delta(w_I - u)|_{2,P} + |\Pi_P^\Delta(u) - u|_{2,P} + |u - w_I|_{2,P} \\
&\leq |\Pi_P^\Delta(u) - u|_{2,P} + 2|u - w_I|_{2,P}.
\end{aligned}
\tag{41}
$$

The first term above is bounded by standard polynomial approximation, while the second one is bounded using (39). We get

$$|\varphi|_{2,P} \lesssim h_P |u|_{3,P}. \tag{42}$$

We are now ready to present the interpolant in the V_h space, that is $u_I = w_I + \varphi$. We first check that $u_I \in V_h$, see definition (15).

- u_I satisfies the conditions at the boundary since φ and $\partial_n \varphi$ vanish at ∂P;

- $\Delta^2 u_I \in \mathbb{P}_2(P)$ since $\Delta^2 w_I = 0$ and we deduce that $\Delta^2 \varphi = -p \in \mathbb{P}_2(P)$ from the first equation of (40);

- It is easy to check that, by definition of Π_P^Δ and integrating by parts, it holds $\Pi_P^\Delta(\varphi) = 0$. Therefore, using the second equation of (40), it immediately follows that, for any $q \in \mathbb{P}_2(P)$,

$$\int_P u_I \, q \, \mathrm{dP} = \int_P (w_I + \varphi) \, q \, \mathrm{dP} = \int_P \Pi_P^\Delta(w_I) \, q \, \mathrm{dP} = \int_P \Pi_P^\Delta(u_I) \, q \, \mathrm{dP}.$$

Therefore $u_I \in V_h$ since it satisfies all conditions in the definition. Finally, the result follows from (39) and (42)

$$|u - u_I|_{2,P} \leq |u - w_I|_{2,P} + |\varphi|_{2,P} \lesssim h_P |u|_{3,P}.$$

$\square$

Corollary 5.3. *Let $u \in H^3(\Omega)$ and u_I the only function in V_h that interpolates the nodal values of u and ∇u at all vertexes of Ω_h. Then it holds*

$$|u - u_I|_{m,\Omega} \lesssim h^{3-m}|u|_{3,\Omega_h} \quad for \ m = 0, 1.$$

Proof. Let U_h denote the standard C^0 virtual element space of order 1 in 3D (see for instance [1, 9]). The degrees of freedom of such space are simply given by the value at all mesh vertexes. Let $\psi_I \in U_h$ be the unique vertex interpolant of $(u - u_I)$. Since $u - w_I$ vanishes at all vertexes, $\psi_I = 0$. Therefore, also using approximation estimates for C^0 virtual element spaces in 3D (see for instance [30, 24]), we get

$$|u - u_I|_{m,\Omega} = |(u - u_I) - \psi_I|_{m,\Omega} \lesssim h^{2-m}|u - u_I|_{2,\Omega}$$

The result follows using Proposition 5.2. $\qquad\square$

Remark 5.2. *The above results could be easily extended to the case with lower regularity $u \in H^s$, $s > 5/2$, since in such case the above interpolants are still well defined. Instead, extending to the case $u \in H^s$ with $2 < s < 5/2$ would require a different kind of interpolation (in the Clément or Scott-Zhang spirit).*

6. Numerical results

In this section we numerically validate the theory behind the C^1 virtual elements proposed in this paper.

6.1. Domain discretization

We will consider two different computational domains: the standard unit cube $[0, 1]^3$ and the truncated octahedron [58]. We discretize such geometries in three different ways.

- **Structured**: the computational domain is decomposed by cubes inside the domain and arbitrary shaped polyhedron close to the boundary, see Figure 2 (a). When we take the unit cube as domain, this type of mesh becomes a standard structured decomposition composed by small cubes.

- **Tetra**: a Delaunay tetrahedral mesh of the input domain, see Figure 2 (b).

- **CVT**: the domain is discretized via a Centroidal Voronoi Tessellation, i.e. a Voronoi tessellation where the centroid of the Voronoi cells coincides with the control points of the cells. This kind of mesh can be computed via a standard Lloyd algorithm [33]. In Figure 2 (c) we show a CVT discretization of the truncated octahedron geometry.

- **Random**: refers to a Voronoi tessellation where we randomly distributed the control points of the cells inside the domain and we do not make any optimization on cells' shape, see Figure 2 (d).

In order to build such meshes we exploit the c++ library `voro++` [52] and follow the strategies described in [9], while for tetrahedral meshes we use `tetgen` [53]. We construct a sequence of meshes for each type and we define the mesh-size as
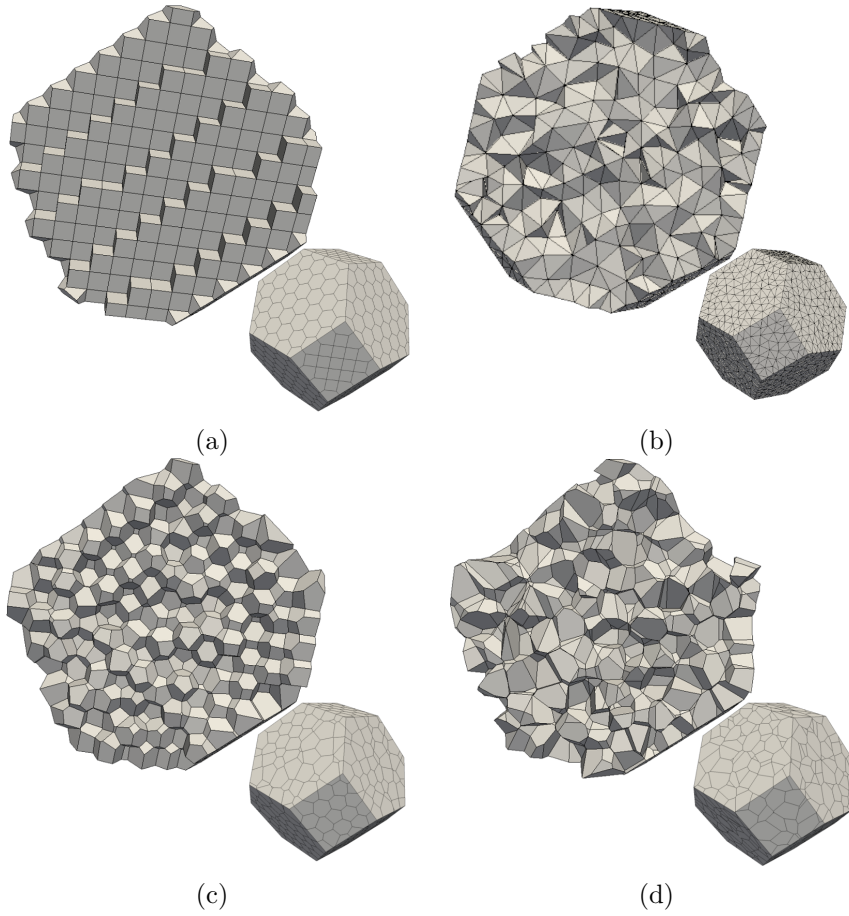
$$h := \frac{1}{n_P} \sum_{P \in \Omega_h} h_P \,,$$

Figure 2: Truncated octahedron geometries with Structured (a), tetrahedral (b), CVT (c) and Random (d) discretization.

where n_P is the number of polyhedrons Ω_h.

We underline that the **Random** partitions are particularly interesting from the computational point of view. Indeed, such meshes contains small edges/faces and stretched polyhedrons so the robustness of the virtual element method will be severely tested.

6.2. Error norms

Suppose that u is the exact solution of the partial differential equation we are solving and let u_h be the discrete solution provided by VEM. We consider the following error quantities:

- **H^2-seminorm relative error:**

$$e_{H^2} := \frac{1}{|u|_{2,\Omega}} \left(\sum_{P \in \Omega}^{n_P} |u - \Pi_P^\Delta u_h|_{2,P}^2 \right)^{1/2},$$

where Π_P^Δ is the $\Delta-$projection operator defined in Equation (12);

18

- H^1-seminorm and L^2-norm relative errors:

$$e_{H^1} \quad := \quad \frac{1}{|u|_{1,\Omega}} \left(\sum_{P \in \Omega}^{n_P} |u - \Pi_P^\nabla u_h|_{1,P}^2 \right)^{1/2} ,$$

$$e_{L^2} \quad := \quad \frac{1}{||u||_{2,\Omega}} \left(\sum_{P \in \Omega}^{n_P} ||u - \Pi_P^0 u_h||_{2,P}^2 \right)^{1/2} ,$$

where Π_P^∇ and Π_P^0 are the operators defined in Equations (22) and (20), respectively;

- l^∞-**type relative error:** We consider the l^∞-type error for functions and gradients

$$e_{l^\infty} \quad := \quad \frac{\max_{\nu \in \Omega_h} |u(\nu) - u_h(\nu)|}{\max_{\nu \in \Omega_h} |u(\nu)|}$$

$$e_{l^\infty}^\nabla \quad := \quad \frac{\max_{\nu \in \Omega_h} ||\nabla u(\nu) - \nabla u_h(\nu)||_\infty}{\max_{\nu \in \Omega_h} ||\nabla u(\nu)||_\infty} ,$$

where $|| \cdot ||_\infty$ is the standard l^∞ norm of three dimensional vectors.

6.3. Numerical experiments

In the following three Sections we develop three different experiments to validate the proposed method. First of all we show a convergence analysis of the method, Section 6.4. Then, we analyze different choices of the scaling parameter h_ν, Section 6.5. Finally we compare this method with the standard C^0 VEM approach proposed in [9], Section 6.6.

The numerical scheme was developed inside the `vem++` library, a `c++` code built at the University of Milano - Bicocca during the CAVE project (https://sites.google.com/view/vembic/home).

6.4. Example 1: Bi-Laplacian with reaction, $h-$convergence analysis

Let Ω be the truncated octahedron, we consider the following partial differential equation

$$\begin{cases} \Delta^2 u + u &= f & \text{in } \Omega \\ u &= g_1 & \text{on } \partial\Omega \\ \partial_n u &= g_2 & \text{on } \partial\Omega \end{cases} , \tag{43}$$

the right hand side f and the Dirichlet boundary conditions g_1 and g_2 are chosen in such a way that the solution of Equation (43) is

$$u(x, y, z) := \sin(\pi xyz) .$$

In the present test we take as parameter h_ν the mean value of the diameters of all polyhedrons which share the mesh vertex ν, a quite natural choice, see Section 3.4.

In Figure 3 we show the convergence lines for the errors in the H^2-seminorm and L^2-norm. The trend of the H^2-seminorm error is the expected one, see
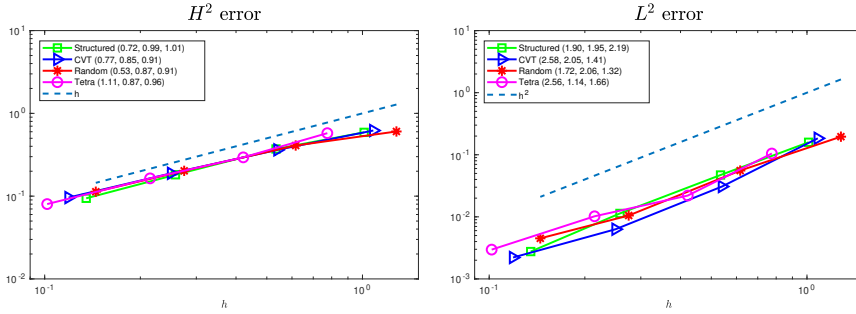
Figure 3: Example 1: convergence lines of e_{H^2} (left) and e_{L^2} (right) for the **Structured**, **Tetra**, **CVT** and **Random**. In the legend we report the convergence order at each step.

Theorem 5.1, i.e. it is approximately of order 1. The convergence lines of the each type of mesh are close to each other.

In Figure 4 we show the trend of the errors e_{l^∞} and $e_{l^\infty}^\nabla$. We did not derive a theoretical proof about the trend of such errors, but we can empirically deduce from these graphs that the convergence rate of e_{l^∞} is between 2 and 3 while the one of $e_{l^\infty}^\nabla$ is 2.
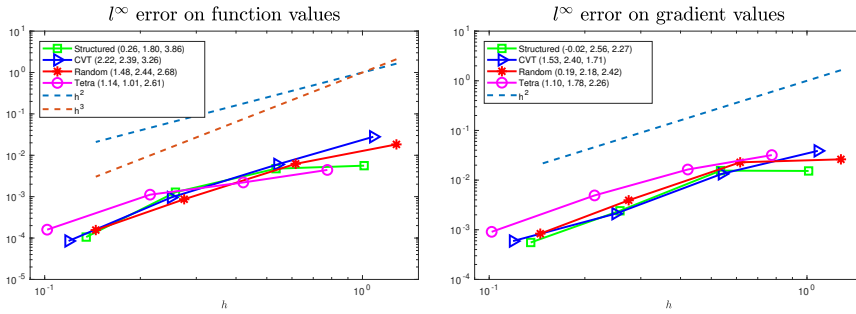

Figure 4: Example 1: convergence lines of e_{l^∞} (left) and $e_{l^\infty}^\nabla$ (right) for the **Structured**, **Tetra**, **CVT** and **Random**. In the legend we report the convergence order at each step.

6.5. Example 2: analysis on h_ν

In the present section we investigate different choices of the "local mesh size" scaling parameter h_ν introduced in Section 3.4, see in particular Equation (25). We consider the following problem

$$
\begin{cases}
\Delta^2 u = f & \text{in } \Omega \\
u = g_1 & \text{on } \partial\Omega \backslash \Gamma \\
\partial_n u = g_2 & \text{on } \partial\Omega \backslash \Gamma \quad, \\
\Delta u = 0 & \text{on } \Gamma \\
-\partial_n \Delta u = 0 & \text{on } \Gamma
\end{cases}
\tag{44}
$$

where Ω is the standard unit cube, Γ are the faces associated with the planes $x = 0$ and $x = 1$, where we apply homogeneous Neumann boundary conditions,

20

f, g_1 and g_2 are chosen in such a way that the exact solution is the function

$$u(x,\, y,\, z) = \frac{1}{12}\, x^4 y\, z\,.$$

Before showing the numerical results, we explain the choices we made for the scaling parameter h_ν. Given a vertex ν of a mesh, we temporary use the following labels to denote these three collections of diameters:

- h_P the diameter of all polyhedrons sharing ν;

- h_f the diameter of all faces sharing ν;

- h_e the diameter of all edges whose endpoint is ν.

Then we can take the mean, the maximum or the minimum of these set of diameters to associate with ν a unique scalar value h_ν. These operations give a total of $3 \times 3 = 9$ possible choices for h_ν. For instance, the label max h_f means that we take as h_ν the maximum (max) diameter among all the faces (h_f) sharing ν.

We take into account only the set of **CVT** and **Random** meshes, because in a structured mesh these choices of h_ν are really close to each other.

In Figures 5 and 6 we show the convergence lines for the set of **CVT** and **Random** meshes, respectively.

The trend of the H^2-seminorm error is similar for each choice of the scaling parameter h_ν, indeed the convergence lines are all indistinguishable except for the minimum h_e choice, (exhibiting the worst behavior), see Figures 5 and 6 left.

The behavior of the L^2-norm error is more sensitive with respect to the parameter h_ν but it preserves a similar slope of the error in all cases. Also in this case the minimum h_e presents a worse behavior with respect to all the other ones.
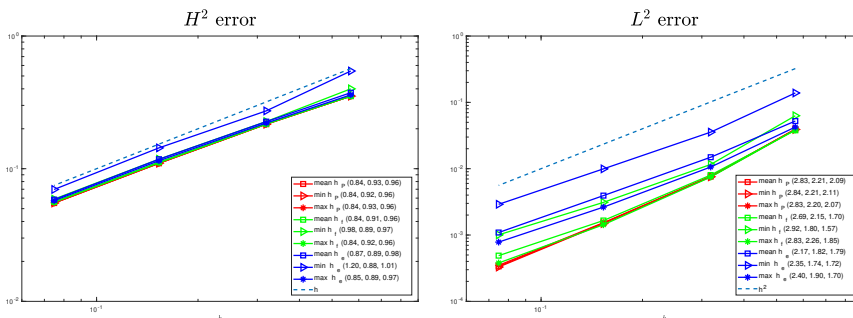

Figure 5: Example 2: trend of the H^2-seminorm (left) and L^2-norm (right) error with different scaling parameter h_ν for **CVT** meshes. In the legend we report the convergence order at each step.

6.6. Example 3: Comparison with C^0 VEM approach

In this section we consider the same test of Section 3.3 in [9]. We take the truncated octahedron as domain and we solve the following second order partial
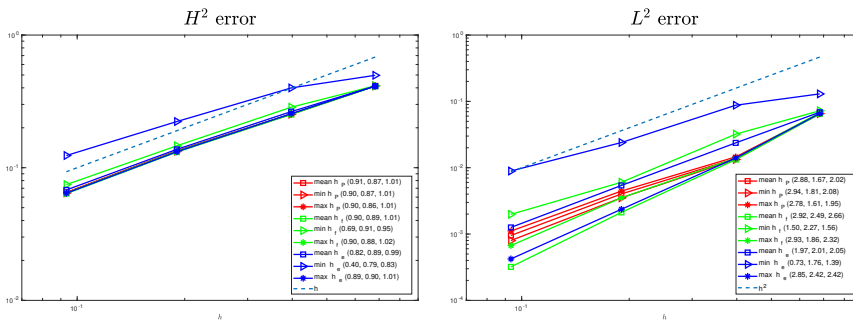
Figure 6: Example 2: trend of the H^2-seminorm (left) and L^2-norm (right) error with different scaling parameter h_ν for **Random** meshes. In the legend we report the convergence order at each step.

differential equation

$$\begin{cases} -\Delta u + u & = & f & \text{in } \Omega \\ u & = & g_1 & \text{on } \partial\Omega \end{cases}, \tag{45}$$

and we choose the right hand side f and g_1 in such a way that the exact solution is

$$u(x,\, y,\, z) := \sin(2xy)\,\cos(z)\,.$$

We consider three "different" C^0 VEM schemes of degree 2 in 3D which differ in the number of degrees of freedom. More specifically, given a mesh composed by n_P polyhedrons, n_f faces, n_e edges and n_ν vertices, we consider the following choices of C^0 or C^1 VEM approaches

- **c1**: the C^1 method proposed in this paper,

$$\#dofs = 4n_\nu\,,$$

- **c0**: a standard C^0 VEM [9],

$$\#dofs = n_\nu + n_e + n_f + n_P\,,$$

- **c0 static cond**: a standard C^0 VEM with static condensation of the internal-to-element degrees of freedom,

$$\#dofs = n_\nu + n_e + n_f\,,$$

- **c0 sere**: a serendipity C^0 VEM with static condensation [14],

$$\#dofs = n_\nu + n_e\,.$$

The mesh-size parameter behaves as $h \sim \#dofs^{-1/3}$ so the theoretical slope in a $\#dof$ vs H^1-seminorm error graph is expected to be $-2/3$ in all cases (that corresponds to $O(h^2)$ convergence rate).

In Figure 7 we show the convergence lines of the H^1-seminorm error for the set of meshes **CVT** and **Random** in terms of number of degrees of freedom.

22

From these convergence lines, we numerically show that all these methods have the expected error trend. Moreover, we observe that the error values at each step are close to each other for all methods.

We also observe that for a given level of accuracy, the number of degrees of freedom to get a C^1 solution is approximately the same as for a C^0 scheme; clearly, the number of degrees of freedom is only a rough indicator of the overall computational cost.
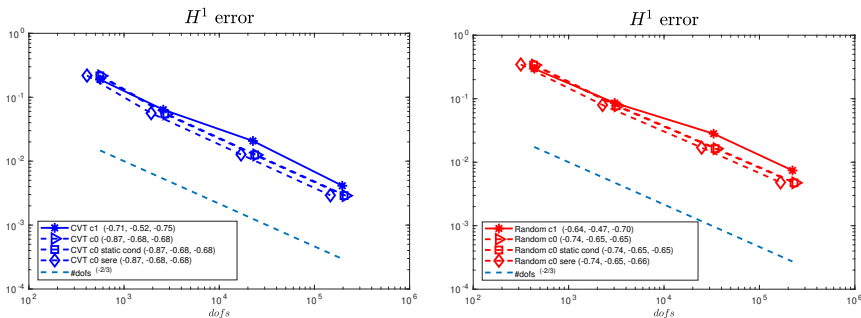

Figure 7: Example 3: trend of the H^1-seminorm error with **CVT** (left) and **Random** (right) meshes. In the legend we report the convergence order at each step.

As a final comparison, we compare the running times (in seconds) for the C^1 scheme and the C^0 schemes (original and Serendipity version). The considered problem is (45) and the adopted meshes are the CVT and random Voronoi. The results are reported in Table 1, where we present both the the assembling and solving time. The code is runned in serial on a Linux machine with processor Intel(R) Xeon(R) CPU E5-2637 v4 @ 3.50GHz. The solution of the linear system is obtained via the direct solver provided by Pardiso [43]. We underline that the involved times could be reduced by running the whole code (both assembling and solving) in parallel, but this is beyond the scope of the present work.

From such data we observe that, as expected, both the assembling and solving time of **c1** is sensibly greater than the other types. Indeed the C^1 scheme involves a more complex structure in terms of degrees of freedom and projection operators, in addition to having slightly more DoFs. On the other hand, this is only a rough time comparison based on our current C++ code; optimizing the codes could lead to smaller differences. We also remind that the purpose of the C^1 scheme is on fourth order problems, and here we are only checking its performance on second order problems (for which it seems a viable, but not optimal, choice).

Acknowledgments

	c1		c0		c0 sere	
	T_{ass}	T_{sol}	T_{ass}	T_{sol}	T_{ass}	T_{sol}
CVT 1	1	≈ 0	≈ 0	≈ 0	≈ 0	≈ 0
CVT 2	5	≈ 0	1	≈ 0	≈ 0	≈ 0
CVT 3	8	160	5	3	5	2
CVT 4	1695	854	49	208	44	98

	c1		c0		c0 sere	
	T_{ass}	T_{sol}	T_{ass}	T_{sol}	T_{ass}	T_{sol}
Random 1	≈ 0	1	≈ 0	≈ 0	≈ 0	≈ 0
Random 2	7	1	1	≈ 0	≈ 0	≈ 0
Random 3	74	11	8	8	7	4
Random 4	884	641	59	325	52	145

Table 1: Example 3, time comparison among C^1 and C^0 VEM. Assembling time in seconds, T_{ass}, and solving time in seconds, T_{sol}, for different meshes of the CVT and Random Voronoi families.

Appendix A. A glimpse to the general order case

In this appendix we give an hint on the general order case $k > 2$, the lowest order case presented in the paper corresponds to $k = 2$. We limit ourself to the definition of the local face and polyhedral spaces, i.e. we consider the same work-flow of Section 3 but omit the proof of these results which can be deduced from the lowest order case.

Starting from the functional spaces defined in the following paragraphs, the generalization of the discrete forms defined in Equation (26) becomes technical but straightforward.

To define such functional spaces, we define the polynomial space $\mathbb{P}_s\backslash\mathbb{P}_r(\mathcal{D})$ as any complement space of $\mathbb{P}_r(\mathcal{D})$, i.e. that verifies

$$\mathbb{P}_s(\mathcal{D}) = (\mathbb{P}_s\backslash\mathbb{P}_r(\mathcal{D})) \oplus \mathbb{P}_r(\mathcal{D}),$$

where $\mathcal{D}$ is a generic two or three dimensional domain and the integers $s > r \geq 0$.

Virtual element nodal space $V_{h,k}^\nabla(f)$

We start from the preliminary space

$$\widetilde{V}_{h,k}^\nabla(f) := \left\{ v_h \in H^1(f) \quad : \quad \Delta_\tau v_h \in \mathbb{P}_{k-2}(f), \right.$$
$$\left. v_h|_{\partial f} \in C^0(\partial f), \ v_h|_e \in \mathbb{P}_{k-1}(e) \ \forall e \in \partial f \right\}.$$

We build the projection operator $\Pi_{f,k}^\nabla : \widetilde{V}_{h,k}^\nabla(f) \to \mathbb{P}_{k-1}(f)$, defined in a similar way as in Equation (4), and the functional space

$$V_{h,k}^\nabla(f) := \left\{ v_h \in V_{h,k}^\nabla(f) \ : \ \int_f \Pi_{f,k}^\nabla v_h \, q \, \mathrm{d}f = \int_f v_h \, q \, \mathrm{d}f, \quad \forall q \in \mathbb{P}_{k-2}\backslash\mathbb{P}_{k-3}(f) \right\}.$$

The degrees of freedom of such space are the standard nodal VEM ones and they are enough to define $\varPi_{f,k}^{\nabla}$. This virtual element space is standard in the virtual element community, we refer to [12] for more details.

Virtual element C^1 space $V_{h,k}^{\Delta}(f)$

We generalize the preliminary space defined in Subsection 3.2 as

$$\widetilde{V}_{h,k}^{\Delta}(f) := \left\{ v_h \in H^2(f) \quad : \quad \begin{aligned} &\Delta_\tau^2 \, v_h \in \mathbb{P}_{k-1}(f), \\ &v_h|_{\partial f} \in C^0(\partial f), \ v_h|_e \in \mathbb{P}_k(e) \ \forall e \in \partial f, \\ &\nabla_\tau \, v_h|_{\partial f} \in [C^0(\partial f)]^2, \\ &\partial_{n_e} v_h \in \mathbb{P}_{k-1}(e) \ \forall e \in \partial f \end{aligned} \right\},$$

Starting from the projection operator $\varPi_{f,k}^{\Delta} : \widetilde{V}_{h,k}^{\Delta}(f) \to \mathbb{P}_k(f)$ defined in a similar way as $\varPi_f^{\Delta}$, see Equation (6), we are able to define the virtual space

$$V_{h,k}^{\Delta}(f) := \left\{ v_h \in \widetilde{V}_{h,k}^{\Delta}(f) \ : \ \int_f \varPi_{f,k}^{\Delta} v_h \ q \, \mathrm{d}f = \int_f v_h \ q \, \mathrm{d}f, \quad \forall q \in \mathbb{P}_{k-1} \backslash \mathbb{P}_{k-4}(f) \right\},$$

Also in this case the degrees of freedom are enough to define $\varPi_{f,k}^{\Delta}$. This space face is similar to the one defined in [18] and we refer to this paper for more details.

Moreover, it is easy to show that starting from the degrees of freedom of $V_{h,k}^{\Delta}(f)$, it is possible to define the L^2 projection operator to approximate the gradient of a function $v_h \in V_{h,k}^{\Delta}(f)$, i.e. $\boldsymbol{\varPi}_{f,k-1}^0$ (the counterpart of the operator defined in Equation (10)).

General order virtual element space in P

Given a polyhedron $P \in \Omega_h$ we consider the preliminary space

$$\widetilde{V}_{h,k}(P) := \left\{ v_h \in H^2(P) \quad : \quad \begin{aligned} &\Delta^2 \, v_h \in \mathbb{P}_k(P), \\ &v_h|_{S_P} \in C^0(S_P) \,, \nabla v_h|_{S_P} \in [C^0(S_P)]^3 \,, \\ &v_h|_f \in V_{h,k}^{\Delta}(f) \,, \partial_{n_f} v_h|_f \in V_{h,k}^{\nabla}(f) \quad \forall f \in \partial P \end{aligned} \right\},$$

In this virtual element space we define the following set of linear operators from $\widetilde{V}_{h,k}(P)$ to $\mathbb{R}$:

D0: the values of the function at the vertices, $v_h(\nu)$;

D1: the values of the gradient components at the vertices, $\nabla v_h(\nu)$;

D2: values of $v_h(\nu)$ at $\max\{k-3,0\}$ internal points for each edge of ∂P;

D3: values of $\nabla v_h(\nu)$ along two normal-to-edge directions at $k-2$ internal points for each edge of ∂P;

D4: for each face $f \in \partial P$ we define the function moments

$$\int_f v_h\, q\, \mathrm{d}f \qquad \forall q \in \mathbb{P}_{k-4}(f)\,,$$

D5: for each face $f \in \partial P$ we define the gradient moments

$$\int_f (\nabla v_h \cdot \mathbf{n}_f)\, q\, \mathrm{d}f \qquad \forall q \in \mathbb{P}_{k-3}(f)\,,$$

D6: the internal function moments

$$\int_P v_h\, q\, \mathrm{d}f \qquad \forall q \in \mathbb{P}_{k-4}(P)\,.$$

Starting from these linear operators it is possible to determine the projection operator $\Pi^{\Delta}_{P,k} : \widetilde{V}_h(P) \to \mathbb{P}_k(P)$ defined in a similar way as in Equation (12). It is easy to see that this projection operator is uniquely defined by $\mathbf{D1} - \mathbf{D6}$ through the face projectors $\Pi^{\nabla}_{f,k}$, $\Pi^{\Delta}_{f,k}$ and $\boldsymbol{\Pi}^0_{f,k-1}$. Then the C^1 general order virtual elements space defined on polyhedron reads

$$V_h(P) \;:=\; \left\{ v_h \in \widetilde{V}_{h,k}(P) \;:\; \int_P \Pi^{\Delta}_{P,k} v_h\; q\, \mathrm{d}P = \int_P v_h\; q\, \mathrm{d}P\,, \quad \forall q \in \mathbb{P}_k \backslash \mathbb{P}_{k-4}(P) \right\}.$$

References

[1] B. Ahmad, A. Alsaedi, F. Brezzi, L. D. Marini, and A. Russo. Equivalent projectors for virtual element methods. *Comput. Math. Appl.*, 66(3):376–391, 2013.

[2] P. F. Antonietti, L. Beirão Da Veiga, D. Mora, and M. Verani. A stream virtual element formulation of the stokes problem on polygonal meshes. *SIAM J. Numer. Anal.*, 52(1):386–404, 2014.

[3] P. F. Antonietti, L. Beirão da Veiga, S. Scacchi, and M. Verani. A C^1 virtual element method for the Cahn-Hilliard equation with polygonal meshes. *SIAM J. Numer. Anal.*, 54(1):34–57, 2016.

[4] D. N. Arnold and F. Brezzi. Mixed and nonconforming finite element methods : implementation, postprocessing and error estimates. *ESAIM: M2AN*, 19(1):7–32, 1985.

[5] E. Artioli. Asymptotic homogenization of fibre-reinforced composites: a virtual element method approach. *Meccanica*, 53(6):1187–1201, 2018.

[6] E. Artioli, S. de Miranda, C. Lovadina, and L. Patruno. A family of virtual element methods for plane elasticity problems based on the Hellinger–Reissner principle. *Comput. Methods Appl. Mech. Engrg.*, 340:978 – 999, 2018.

[7] A. Barton and S. Mayboroda. Higher-order elliptic equations in non-smooth domains: history and recent results. *Harmonic Analysis, Partial Differential Equations, Complex Analysis, Banach Spaces, and Operator Theory*, 1(4):55–121, 2016.

[8] L. Beirão da Veiga, F. Brezzi, L. D. Marini, and A. Russo. The hitchhiker's guide to the virtual element method. *Math. Models Methods Appl. Sci.*, 24(08):1541–1573, 2014.

[9] L. Beirão da Veiga, F. Dassi, and A. Russo. High-order virtual element method on polyhedral meshes. *Comput. Math. Appl.*, 74(5):1110–1122, 2017.

[10] L. Beirão da Veiga, C. Lovadina, and D. Mora. A virtual element method for elastic and inelastic problems on polytope meshes. *Comput. Methods Appl. Mech. Engrg.*, 295:327–346, 2015.

[11] L. Beirão da Veiga, D. Mora, and G. Rivera. Virtual elements for a shear-deflection formulation of Reissner–Mindlin plates. *Math. Comp.*, 2018.

[12] L. Beirão da Veiga, F. Brezzi, A. Cangiani, G. Manzini, L. D. Marini, and A. Russo. Basic principles of virtual element methods. *Math. Models Methods Appl. Sci.*, 23(1):199–214, 2013.

[13] L. Beirão da Veiga, F. Brezzi, F. Dassi, L. D. Marini, and A. Russo. Lowest order virtual element approximation of magnetostatic problems. *Comput. Methods Appl. Mech. Engrg.*, 332:343–362, 2018.

[14] L. Beirão Da Veiga, F. Brezzi, F. Dassi, L. D. Marini, and A. Russo. Serendipity virtual elements for general elliptic equations in three dimensions. *Chinese Annals of Mathematics, Series B*, 39(2):315–334, Mar 2018.

[15] L. Beirão da Veiga, F. Brezzi, L. D. Marini, and A. Russo. Virtual element method for general second-order elliptic problems on polygonal meshes. *Math. Models Methods Appl. Sci.*, 26(04):729–750, 2016.

[16] L. Beirão da Veiga, C. Lovadina, and A. Russo. Stability analysis for the virtual element method. *Math. Models Methods Appl. Sci.*, 27(13):2557–2594, 2017.

[17] L. Beirão da Veiga, C. Lovadina, and G. Vacca. Virtual elements for the Navier–Stokes problem on polygonal meshes. *SIAM J. Numer. Anal.*, 56(3):1210–1242, 2018.

[18] L. Beirão da Veiga and G. Manzini. A virtual element method with arbitrary regularity. *IMA J. Numer. Anal.*, 34(2):759–781, 2014.

[19] M. F. Benedetto, S. Berrone, A. Borio, S. Pieraccini, and S. Scialò. A hybrid mortar virtual element method for discrete fracture network simulations. *J. Comput. Phys.*, 306:148–166, 2016.

[20] M. F. Benedetto, S. Berrone, S. Pieraccini, and S. Scialò. The virtual element method for discrete fracture network simulations. *Comput. Methods Appl. Mech. Engrg.*, 280:135–156, 2014.

[21] S. Bertoluzza, M. Pennacchio, and D. Prada. Bddc and feti-dp for the virtual element method. *Calcolo*, 54(4):1565–1593, 2017.

[22] D. Boffi, F. Brezzi, and M. Fortin. *Mixed finite element methods and applications*, volume 44 of *Springer Series in Computational Mathematics*. Springer, Heidelberg, 2013.

[23] L. Botti, D. A. Di Pietro, and J. Droniou. A hybrid high-order discretisation of the brinkman problem robust in the darcy and stokes limits. *Comput. Methods Appl. Mech. Engrg.*, 341:278 – 310, 2018.

[24] S. C. Brenner, Q. Guan, and Li-Y. Sung. Some estimates for virtual element methods. *Comput. Methods Appl. Math.*, 17(4):553–574, 2017.

[25] S. C. Brenner and L. R. Scott. *The mathematical theory of finite element methods*, volume 15 of *Texts in Applied Mathematics*. Springer, New York, third edition, 2008.

[26] S. C. Brenner and Li-Y. Sung. C^0 interior penalty methods for fourth order elliptic boundary value problems on polygonal domains. *J. Sci. Comput.*, 22/23:83–118, 2005.

[27] S. C. Brenner and Li-Y. Sung. Virtual element methods on meshes with small edges or faces. *Math. Models Methods Appl. Sci.*, 28(07):1291–1336, 2018.

[28] F. Brezzi and L. D. Marini. Virtual element methods for plate bending problems. *Comput. Methods Appl. Mech. Engrg.*, 253:455–462, 2013.

[29] E. Cáceres and G. N. Gatica. A mixed virtual element method for the pseudostress–velocity formulation of the stokes problem. *IMA J. Numer. Anal.*, 37(1):296–331, 2017.

[30] A. Cangiani, E. H. Georgoulis, T. Pryer, and O. J. Sutton. A posteriori error estimates for the virtual element method. *Numer. Math.*, 137(4):857–893, 2017.

[31] A. Cangiani, V. Gyrya, and G. Manzini. The nonconforming virtual element method for the stokes equations. *SIAM J. Numer. Anal.*, 54(6):3411–3435, 2016.

[32] F. Dassi and L. Mascotto. Exploring high-order three dimensional virtual elements: bases and stabilizations. *Comput. Math. Appl.*, 75(9):3379–3401, 2018.

[33] Q. Du, V. Faber, and M. Gunzburger. Centroidal voronoi tessellations: Applications and algorithms. *SIAM Rev.*, 41(4):637–676, 1999.

[34] G. Engel, K. Garikipati, T. J. R. Hughes, M. G. Larson, L. Mazzei, and R. L. Taylor. Continuous/discontinuous finite element approximations of fourth-order elliptic problems in structural and continuum mechanics with applications to thin beams and plates, and strain gradient elasticity. *Comput. Methods Appl. Mech. Engrg.*, 191(34):3669–3750, 2002.

[35] R. Falk. Approximation of the biharmonic equation by a mixed finite element method. *SIAM J. Numer. Anal.*, 15(3):556–567, 1978.

[36] A. Fumagalli and E. Keilegavlen. Dual virtual element method for discrete fractures networks. *SIAM J. Sci. Comput.*, 40(1):B228–B258, 2018.

[37] A. L. Gain, G. H. Paulino, L. S. Duarte, and I.F.M. Menezes. Topology optimization using polytopes. *Comput. Methods Appl. Mech. Engrg.*, 293:411–430, 2015.

[38] A. L. Gain, C. Talischi, and G. H. Paulino. On the virtual element method for three-dimensional linear elasticity problems on arbitrary polyhedral meshes. *Comput. Methods Appl. Mech. Engrg.*, 282:132–160, 2014.

[39] V. Girault and P.A. Raviart. *Finite element methods for Navier-Stokes equations: theory and algorithms*. Springer series in computational mathematics. Springer-Verlag, 1986.

[40] T. Gudi, N. Nataraj, and A. K. Pani. Mixed discontinuous Galerkin finite element method for the biharmonic equation. *J. Sci. Comput.*, 37(2):139–161, 2008.

[41] J. Guzmán and M. Neilan. Conforming and divergence-free stokes elements on general triangular meshes. *Math. Comp.*, 83(285):15–36, 2014.

[42] J. Hu, Y. Huang, and S. Zhang. The lowest order differentiable finite element on rectangular grids. *SIAM J. Numer. Anal.*, 49(4):1350–1368, 2011.

[43] D. Kourounis, A. Fuchs, and O. Schenk. Towards the next generation of multiperiod optimal power flow solvers. *IEEE Trans. Power Syst.*, PP(99):1–10, 2018.

[44] M. Lai and A. LeMéhauté. A new kind of trivariate C1 macro-element. *Adv. Comput. Math.*, 21(3):273–292, Oct 2004.

[45] P. Monk. A mixed finite element method for the biharmonic equation. *SIAM J. Numer. Anal.*, 24(4):737–749, 1987.

[46] D. Mora, G. Rivera, and R. Rodríguez. A virtual element method for the Steklov eigenvalue problem. *Math. Models Methods Appl. Sci.*, 25(08):1421–1445, 2015.

[47] D. Mora, G. Rivera, and I. Velásquez. A virtual element method for the vibration problem of Kirchhoff plates. *ESAIM: M2AN*, 52(4):1437–1456, 2018.

[48] D. Mora and I. Velásquez. A virtual element method for the transmission eigenvalue problem. *Math. Models Methods Appl. Sci.*, 28(14):2803–2831, 2018.

[49] L. S. D. Morley. The triangular equilibrium element in the solution of plate bending problems. *Aeronautical Quarterly*, 19(2):149–169, 1968.

[50] I. Mozolevski, E. Süli, and P. R. Bösing. *hp*-version a priori error analysis of interior penalty discontinuous Galerkin finite element approximations to the biharmonic equation. *J. Sci. Comput.*, 30(3):465–491, 2007.

[51] V. M. Nguyen-Thanh, X. Zhuang, H. Nguyen-Xuan, T. Rabczuk, and P. Wriggers. A virtual element method for 2d linear elastic fracture analysis. *Comput. Methods Appl. Mech. Engrg.*, 2018.

[52] C. H. Rycroft. Voro++: A three-dimensional voronoi cell library in c++. *Chaos*, 19(4):041111, 2009.

[53] Hang Si. Tetgen, a delaunay-based quality tetrahedral mesh generator. *ACM Trans. Math. Softw.*, 41(2):11:1–11:36, February 2015.

[54] G. Vacca. An H^1-conforming virtual element for darcy and brinkman equations. *Math. Models Methods Appl. Sci.*, 28(01):159–194, 2018.

[55] J. Volker, A. Linke, C. Merdon, M. Neilan, and L. G. Rebholz. On the divergence constraint in mixed finite element methods for incompressible flows. *SIAM Review*, 59(3):492–544, 2017.

[56] A. Ženíšek. Polynomial approximation on tetrahedrons in the finite element method. *J. Approx. Theory*, 7:334–351, 1973.

[57] M. Wang and J. Xu. Minimal finite element spaces for $2m$-th-order partial differential equations in R^n. *Math. Comp.*, 82(281):25–43, 2013.

[58] R. Williams. *The Geometrical Foundation of Natural Structure: A Source Book of Design.* Dover Publications, 1979.

[59] P. Wriggers, W.T. Rust, and B.D. Reddy. A virtual element method for contact. *Comput. Mech.*, 58(6):1039–1050, 2016.

[60] S. Zhang. A C1-P2 finite element without nodal basis. *ESAIM: M2AN*, 42(2):175–192, 2008.

[61] J. Zhao, S. Chen, and B. Zhang. The nonconforming virtual element method for plate bending problems. *Math. Models Methods Appl. Sci.*, 26(09):1671–1687, 2016.